SSRG International Journal of Recent Engineering Science
ISSN: 2349–7157 / https://doi.org/10.14445/23497157/IJRES-V11I1P106

Volume 11 Issue 1, 37-43, Jan-Feb 2024

Original Article

Improve the Aerodynamics Performance of the Wing Using Shark Denticles

Masum Hossain[1], Sabbir Hyder[2]

[1]*Department of Aeronautical Engineering, Nanchang Hangkong University.*
[2]*Department of Aeronautical Engineering, Nanjing University of Aeronautics & Astronautics.*

[1]*Corresponding Author : mdadnan57017@gmail.com*

Received: 06 January 2024 Revised: 08 February 2024 Accepted: 19 February 2024 Published: 29 February 2024

Abstract *- Drag reduction has a significant impact on both fuel consumption and an aircraft's aerodynamic performance. The main motive of this paper is to increase the lift and decrease the drag by using shark denticles on the upper surface of the wing with different angles of attack. The shark denticle creates turbulence flow over the wing, and the boundary layer separation in the chord can be extended up to a specified distance. The NACA 0012 airfoil has been utilized to design the wing. After creating the wing, ANSYS 2022 R1 was used to CFD analyze the wing. The SST k-omega turbulence model has used the utilized RANS equation, and Mach 0.6 is assumed as free stream velocity. The findings are noteworthy, and other changes may be necessary to boost performance.*

Keywords *- Shark Denticles, Drag Reduction, Coefficient of Lift, Coefficient of Drag, ANSYS, Wing, Vortex Generators.*

I. Introduction

Drag reduction plays a remarkable role in fuel consumption and aerodynamic performance. It is not only used for fuel consumption and aerodynamic performance of the wing but also it is enhanced the overall performance of the aircraft during take-off, climbing, and gliding.

1.1. Type of Drag

Drag may be classified into three types: i) parasitic drag (which includes form drag and skin friction drag), ii) lift-induced drag, and iii) wave drag. Parasitic drag is a form of aerodynamic drag that acts on any moving object in a fluid. Generate drag and skin friction drag combine to form parasitic drag. It affects all things, regardless of whether they can generate lift. Lift-generated drag is an aerodynamic drag force that develops when a moving object redirects the airflow that is directed at it. This drag force occurs in airplanes because of wings or a lifting body diverting air to generate lift and in automobiles because of airfoil wings redirecting air to cause downforce. Wave Drag is a force or drag that slows the forward velocity of an airplane in both supersonic and transonic flight because of shock wave generation. Researchers and aerodynamicists have worked for decades to increase the lift and decrease the drag. There are some ways researchers work with it, such as creating an inward and outward dimple, using fish scales, using vortice generators, gurney flaps, and using winglets. Aircraft and automobiles are using that system to improve vehicle performance.

Dimples are essentially vortex generators in the form of spherical. It is shaped like a golf ball and has dimples all over the surface. The examination of smooth-surfaced golf balls and dimpled golf balls revealed that the dimpled ball had less drag and goes farther than the smooth ball. The main reason for raising drag by producing a wake zone near the back of the ball is flow separation. Dimples are usually seen on the upper surface of an airfoil at the flow separation point. It keeps the boundary layer together for a longer period, which helps to reduce pressure drag. Dimples reduce drag while simultaneously increasing lift. It generates a turbulent boundary layer by generating vortices because turbulent boundary layers have a smaller wake zone than laminar boundary layers.

We talked about skin friction drag, which occurs when a solid moving object collides with a fluid; as a result of skin friction, a solid object going through fluid experiences drag, which restricts the item's forward motion. We can increase the performance of an item traveling along a fluid flow by lowering skin friction. Aquatic species, such as fish, have adaptations, such as scales on their skin, that help them to travel quicker through the seawater by suffering less drag force. The fish scale has been revealed to contribute to the creation of the turbulent boundary layer.

Vortex Generators are tiny plates that are put on the surface of the wings to modify the flow of air along the wing's surface. The vortex generator's principal application is to produce tiny vortices that hold the flow of air closer to the surface, delaying flow separation. These improve lift while decreasing drag. The vortex generator is most important at low flying speeds, climbs, and high angles of attack. Vortex generators can improve an aircraft's performance and stability. Vortex generators are positioned slantwise to have an angle of attack on the local airflow. Because vortex generators can lower the aircraft's stalling

speed, they can minimize the needed one-engine-inoperative climb performance. Because of the reduced demand for climb performance, the maximum take-off weight can be increased, at least up to the maximum weight allowed by structural standards.

The Gurney flap is a tiny tab that projects from the wing's trailing edge. It is typically positioned at a right angle to the airfoil's pressure-side surface and projects 1% to 2% of the wing chord. This trailing edge device may boost the performance of a basic airfoil to levels comparable to those of complicated high-performance designs.

The device works by raising pressure on the pressure side, lowering pressure on the suction side, and assisting the boundary layer flow in remaining connected to the trailing edge on the suction side of the airfoil. Automobile racing, helicopter horizontal stabilizers, and aircraft where considerable lift is required, such as banner-towing planes, are examples of common usage [11].

Wingtip devices are designed to increase the efficiency of fixed-wing aircraft by reducing drag. Although there are several types of wing tip devices that work in various ways, their intended purpose is always to lower an aircraft's drag by recovering some of the tip vortex energy. Wingtip devices can also improve aircraft handling characteristics and increase safety for the following aircraft. Such devices boost the effective aspect ratio of a wing without significantly extending the wingspan. Extending the span would reduce lift-induced drag while increasing parasitic drag and necessitating an increase in wing strength and weight [12].

1.2. Shark Denticles

Nature has evolved structures and materials whose characteristics frequently serve as inspiration for the design of synthetic systems with unique properties. Shark skin is an example of this, as it is covered with rigid bony denticles (or scales) with a plate-like upper section with ridges that narrow to a thin neck that anchors into the skin [1]. Shark skin is covered by dermal denticles, which are tiny, flat V-shaped scales that look more like teeth than fish scales.

These denticles reduce drag and turbulence, allowing the shark to swim more quickly and quietly. These denticles are all over the skin of the shark. There is a good reason to have these denticles. Different-sized denticles appear to serve different functions. Smaller, thinner denticles reduce surface drag, and sharks can move faster. The thicker one is used for the protection of its own body, providing the shark with a layer of protection against predators and ectoparasites [13].

In this paper, we focus on airfoils and study how shark denticles create lift and decrease drag. Firstly, CFD analysis was conducted in the NACA0012 airfoil. Then, the wings with shark denticles were modelled and analyzed. The NACA0012 airfoil wing and wing with shark denticles performance are compared.

2. Literature Review

Domel A. G., Saadat M., Weaver J. C., Haj-Hariri H., Bertoldi K., & Lauder G. V (2018) have designed a wing that is inspired by the drag reduction properties of the like denticles, which are covered by the skin of a shark and also describe that experimental simulation results into aerodynamics effect of denticles along with a suction side (upper side) of the aerofoil. There is calculated the coefficient of lift, coefficient of drag, and the lift-drag ratio of the wing with different angles of attack [1].

Rajarajan S, Manikandan P, Lokeshkumar K, Surya PL, Syed Masood T S, and Karthikeyan M. (2020) have shown that the drag reduction wing uses a vortex generator, fish scales, and a dimpled ball. All have been done by the subsonic condition using the NACA4412 wing. The coefficient of lift, coefficient of drag, and lift drag ratio are calculated using the different angles of attack (9°, 12°, 15°). In conclusion, after analyzing the wing using different angles of attack, the wing lift increased rapidly and added the components that generated vortex and boundary layer flow from laminar to turbulent [2].

Prithvi Raj Arora, A. Hossain, Prasetyo Edi, A.A. Jaafar, Thamir S. Younis, M. Saleem Thamir S. Younis and M. Saleem (2005), find the aerodynamics characteristic of the aircraft model using NACA653218 wing with elliptical winglet and without elliptical winglet. They were using a subsonic wind tunnel with a 1000mm×1000mm rectangular test section. The 60° inclination is used for the elliptical winglet to get the best performance and provides a 6% improvement in lift curve slope as compared to the San's winglet and the best lift/drag ratio. The addition of an elliptical winglet increases the slope of the lift curve while decreasing drag [3].

Chalia S. & Kumar Bharti M (2017). have shown the manoeuvrability and aerodynamic properties of aircraft, which include reduction of drag, increasing lift, and stalling and delaying flow separation, and shown the design of airfoil with some basic modifications like dimples and vortex generator for increase lift-drag ratio. The wing was simulated using ANSYS software from different attack angles. There are used NACA2412 airfoil's, and in conclusion, the wing lift is increased and drag decreased in different angles of attack [4].

Kousik Kumaar. R, Maniiarasan D. P. (2015) have shown the reduction of drag using riblets on the upper surface of the wing. The turbulent region will produce less drag because the flow transitions from laminar to turbulent around the half chord. The swept wing design in this paper and NASA SC (2) XXXX specification have been used for wing design.

The velocity profiles are determined after measuring the lift, drag, and pressure coefficients. In conclusion, after analyzing the swept wing with riblet and without riblet, the riblet wing creates more lift and less drag compared to the normal wing [5].

Fazle Rabbi M., Nandi R., & Mashud M (2022). The paper shows the design of a wing using NACA0012 airfoil with and without a slotted winglet. The test was carried out in a subsonic wind tunnel with a 1m×1m rectangular test section at a flow speed of 25m/s with the wing without a winglet, the wing with a winglet at 30° inclination, the wing with a winglet at 60° inclination, and the wing with a winglet at 70° inclination at an angle of attack ranging from 0 to 16 degree. The test results show a 20- 25% reduction in drag coefficient and a 10-20% increase in lift coefficient when using a slotted winglet [6].

Rohith I., Rajendran A. R., and Anand D (2019) have shown the method of reducing drag using roughness over the wing surface. Because of that, during the transition, the laminar flow converts turbulence to give less drag. The roughness has reduced viscous drag and increased the coefficient of lift along with the stall angle of attack. For this experiment, NACA0012 airfoil has been used. For the wind tunnel experiment, Al 6061-T6 aluminium alloy was used to fabricate the wing.

The wind tunnel test section is used at 0.3m×0.3m, with an airspeed of 70 m/s and an overall size of 6m. There are calculated coefficients of lift, coefficient of drag, and lift-drag ratio with different angles of attack [7].

Fadl A., Abbasher M., & El Seory (2022) A. investigate the impact of a modified Gurney flap configuration on S823 and S822 aerofoils (from the NREL aerofoil family). The device used is a flap that is 1-3 percent of the length of the aerofoil chord, is oriented perpendicular to the chord line, and is located on the pressure side at 96 percent of the chord from the leading edge. For drag reduction and structural stability, the remaining 4% of the chord was eliminated, like that of blunt trailing edge aerofoils. At different Reynolds numbers, the flow field around the aerofoil was numerically predicted using an incompressible Navier-Stokes solver and the two-equation turbulence model k-ε [8].

3. Methodology

CATIA V5 software is used to create 3D CAD models. CATIA V5 software is the world's leading engineering and design software for 3D CAD product design. It is used in a variety of industries, including aerospace, automotive, consumer goods, and industrial machinery, to design, simulate, analyze, and construct products. After modelling in CATIA V5 software, ANSYS R1 2022 was used for simulation and to calculate the coefficient of lift and coefficient of drag.

ANSYS is a CAE/Multiphysics engineering simulation application that may be used to develop, test, and operate products.

The problem's principal governing equations are continuity and Navier-Stokes equations in their three-dimensional deferential variants.

Continuity Equation [9]: $$\frac{D\rho}{Dt} + \rho\nabla.V = 0 \quad (1)$$

N-V Equation [9]:

$$\rho\frac{Dv}{Dt} = \rho g - \nabla p + \frac{\partial}{\partial x_j}\left[\mu\left(\frac{\partial v_i}{\partial x_j} + \frac{\partial v_j}{\partial x_i}\right) + \lambda\nabla.V\right] \quad (2)$$

Expanding the N-S equation in x, y, and z directions Yields:

x-momentum [9]:

$$\rho\frac{Du}{Dt} = -\frac{\partial p}{\partial x} + \frac{\partial \tau_{xx}}{\partial x} + \frac{\partial \tau_{yx}}{\partial y} + \frac{\partial \tau_{zx}}{\partial z} + \rho f_x \quad (3)$$

y- momentum [9]:

$$\rho\frac{Du}{Dt} = -\frac{\partial p}{\partial x} + \frac{\partial \tau_{xy}}{\partial x} + \frac{\partial \tau_{yy}}{\partial y} + \frac{\partial \tau_{zy}}{\partial z} + \rho f_y \quad (4)$$

z-momentum [10]:

$$\rho\frac{Du}{Dt} = -\frac{\partial p}{\partial x} + \frac{\partial \tau_{xz}}{\partial x} + \frac{\partial \tau_{yz}}{\partial y} + \frac{\partial \tau_{zz}}{\partial z} + \rho f_z \quad (5)$$

From normal and axial force, Lift and Drag can be obtained as [9]:

Lift force: $$L' = N'\cos\alpha - A'\sin\alpha \quad (6)$$

Drag force: $$D' = N'\sin\alpha - A'\cos\alpha \quad (7)$$

The dimensionless force coefficients are defined as follows [9]:

Lift coefficient: $$C_L = \frac{L'}{\frac{1}{2}\rho V^2 c} \quad (8)$$

Drag coefficient: $$C_D = \frac{D'}{\frac{1}{2}\rho V^2 c} \quad (9)$$

4. Geometry Modelling

The performance and operation of any aircraft are fundamentally determined by the type of wing, its parameters, and its characteristics. As a result, the wing of an aircraft is the most important part of its structure.

The aircraft wing is modelled in CATIA V5, and the airfoil coordinates are imported using Microsoft Office Excel Macros. The wing model used in this paper is the NACA0012 airfoil wing, and the angles of attack maintained with the wing model are 9°, 12°, and 15°. The wing model specifications are as follows.

4.1. Properties of the Airfoil

The wing was designed using the NACA0012 airfoil. NACA 0012 indicates that there is no camber or zero camber present, and the maximum thickness of the airfoil is at 12% of the chord from the leading edge.

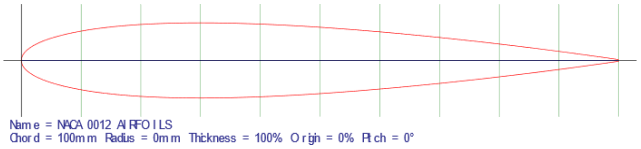

Fig 1. NACA 0012 Airfoil

Table 1. Properties of the airfoil

Airfoil Type	NACA 0012
Chord Length	100 mm
Wingspan	200 mm
Radius	0 mm
Thickness	100%
Origin	0%
Pitch	0°

4.2. Wing With & Without Shark Denticles

The shark denticle is created on the upper surface of the wing in CATIA V5, as shown in the figure. The 27 denticles are used in the row. Each denticle has a maximum thickness of 2mm, and the distance between the denticles from centre to centre is 5mm×5mm. The chord length of the wing is 100mm, and the wingspan is 200mm. For both wings, there are used NACA0012 airfoil.

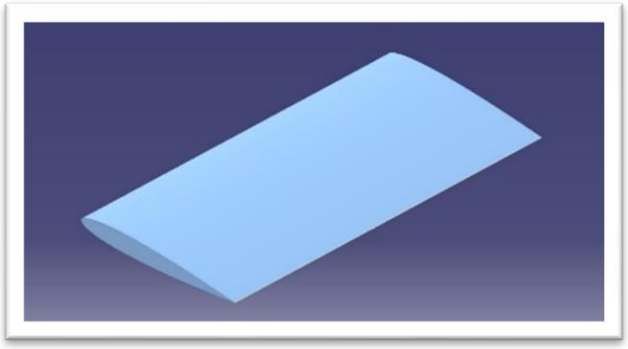

Fig. 2 Wing design

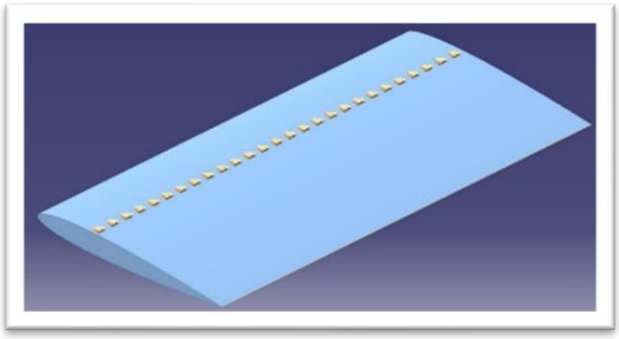

Fig. 3 Wing with shark denticles

5. Analysis

5.1. Meshing

In the engineering process, meshing plays a remarkable role. One of the critical factors for simulation accuracy is the creation of high-quality mesh. The wing was meshed using Ansys Meshing software. Face meshing was used to create a structured mesh and edge sizing was used with the necessary bias to represent the flow and boundary layers accurately throughout the simulation.

The inflation was used to create a better mesh over an airfoil. Inflation meshes are prism layers that are "inflated" from a triangular surface mesh to provide high-quality geometry-aligned components capable of resolving boundary layer growth over the airfoil. The element size used was 0.042 m for the wing and 0.046 for the wing with shark denticles.

Table 2. Mesh validations of wing

Geometry	Nodes	Elements
Wing	102310	479717
Wing with Shark Denticles	120079	493901

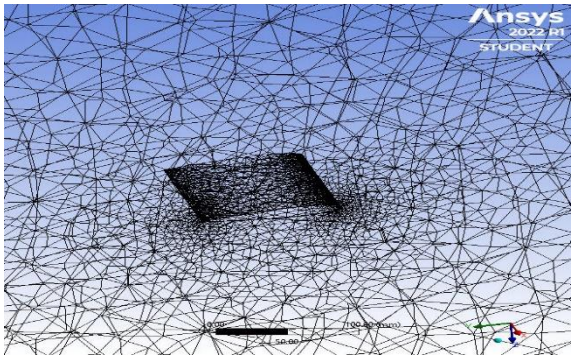

Fig. 4 Generated mesh of the wing

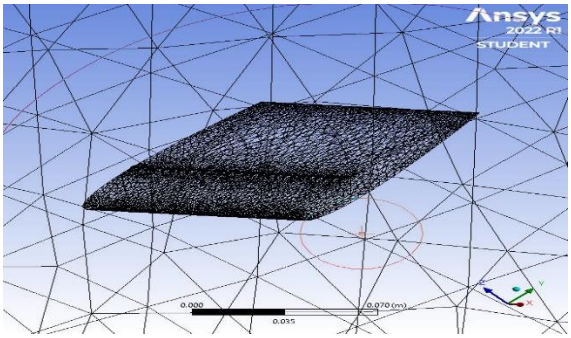

Fig. 5 Generated Mesh of the wing with denticles

5.2. Boundary Condition

Both wings are used same operating condition for analysis where air properties are summarized in the table:

Table 3. Air properties

Properties	Value
Temperature (T)	288.16 K
Pressure (P)	101325 Pa
Density (ρ)	Ideal Gas
Viscosity (μ)	Sutherland
Speed of sound (a)	343 m/s

The wings were tested at a free stream velocity of 206 m/s. The pressure-based solver is used for both wings. The energy Equation was turned on for all the cases, and used the SST k-omega turbulence model for the utilized RANS equation. Each wing was analyzed at Mach 0.6 with 9°,12°, and 15° angles of attack. The inlet is used as a pressure far-field, and the wing is used as a wall for both wings. For the correct solution, the second-order upwind approach is employed for flow, Turbulent Kinetic energy, and turbulent dissipation rate. The configuration was built up utilizing a hybrid initialization procedure based on the pressure inlet value and 800 iterations used for the calculation.

6. Results and Discussion

The wing's pressure contour is presented in Figure 5,7,9, and the wing's turbulence kinetic energy is presented in Figure 6,8,10 with 9°, 12°, and 15° angles of attack.

Those wing studies were performed without any drag reduction components, and the coefficients of lift and drag were calculated at various angles of attack. On the contrary, the wing with denticles in Figure 11,13,15 shows the pressure contour, and Figures 12,14,16 represent the turbulent kinetic energy contour. The wing with denticles creates much lift and less drag compared to the plain wing. The colour of the upper side of the wing represents all the counters of the wing. Blue represents the minimum value, green is the middle, and red is the maximum value. As we see in the graph, graph 1 represents the coefficient of lift vs angle of attack graph. Both wings increase lift at different angles of attack, but the wing with denticles creates more lift than the plain wing. However, Graph 2 shows the coefficient of drag vs angles of attack. This graph shows that the denticles decreased drag more than a normal wing.

6.1. Normal Wing

6.1.1. At Angle of Attack- 9°

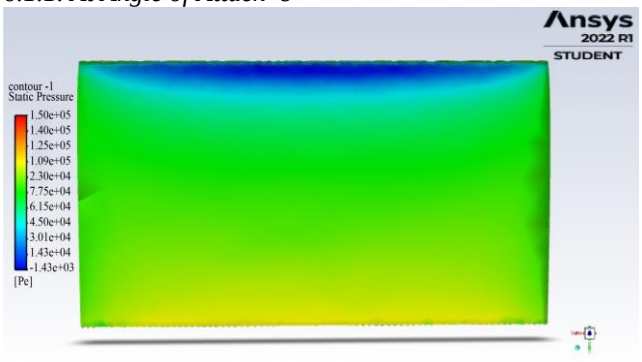

Fig. 6 [Top View] Contour of Pressure

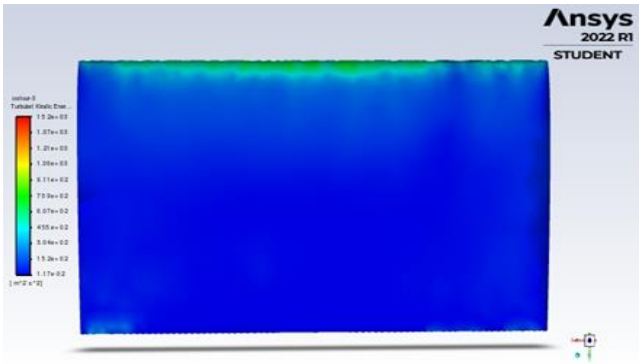

Fig. 7 [Top View] Turbulent kinetic energy

6.1.2. At angle of attack-12°

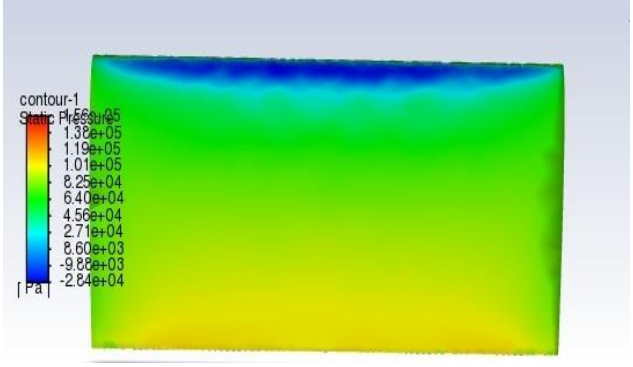

Fig. 8 Pressure contours

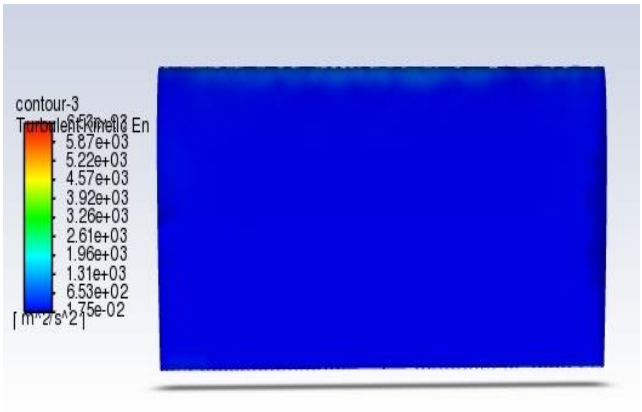

Fig. 9 Turbulent kinetic energy

6.1.3. At Angle of Attack-15°

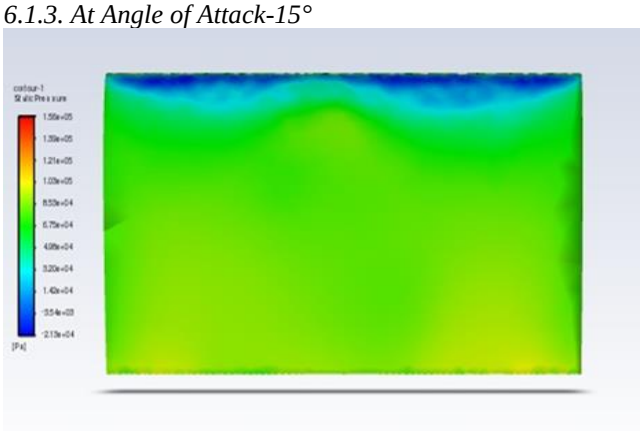

Fig. 10 Pressure contours

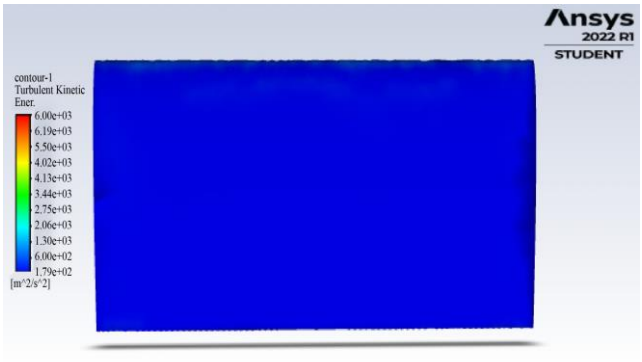

Fig. 11 Turbulent kinetic energy

6.2. Wing with Shark Denticles

6.2.1. At Angle of Attack-9°

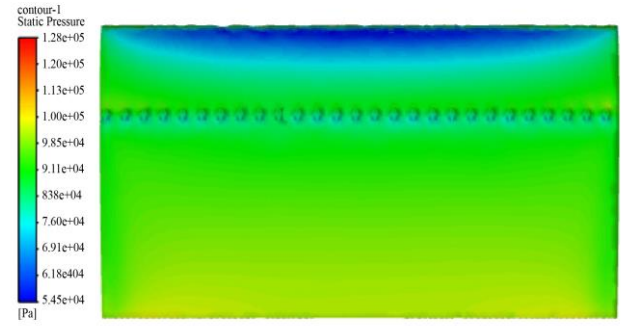

Fig. 12 Pressure contours

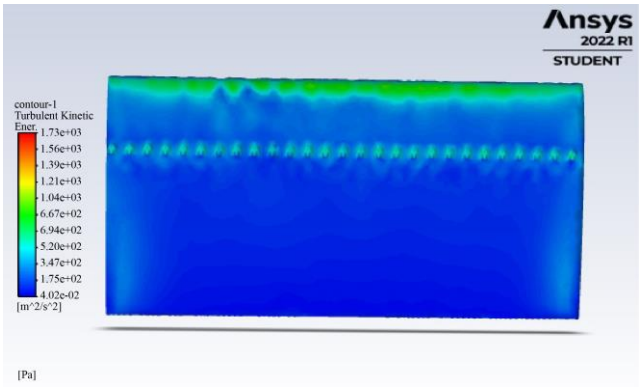

Fig. 13 Turbulent kinetic energy

6.2.2. At Angles of Attack-12°

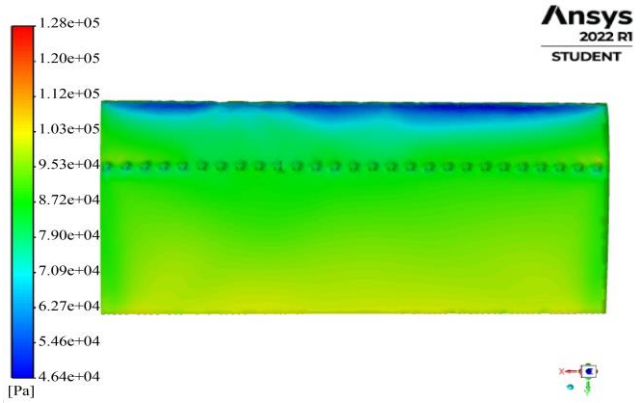

Fig. 14 Pressure contours

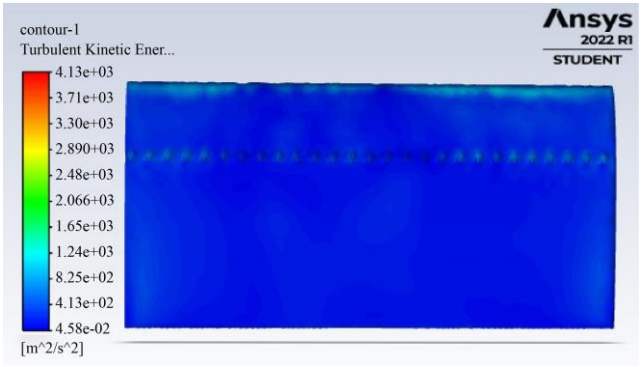

Fig. 15 Turbulent kinetic energy

6.2.3. At angle of attack-15°

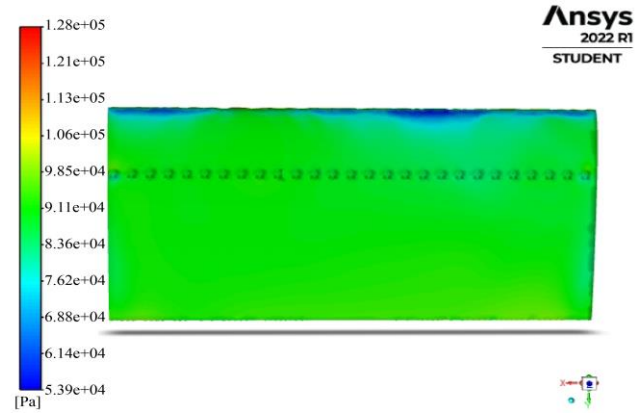

Fig. 16 Pressure contours

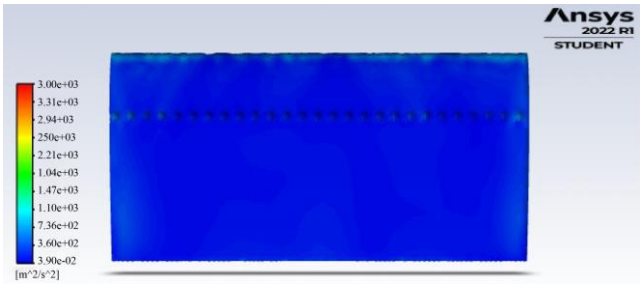

Fig. 17 Turbulent kinetic energy

6.3. Comparison-Graphs

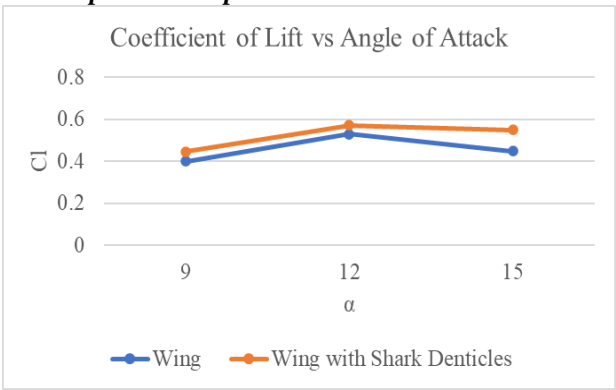

Graph 1. Cl vs α

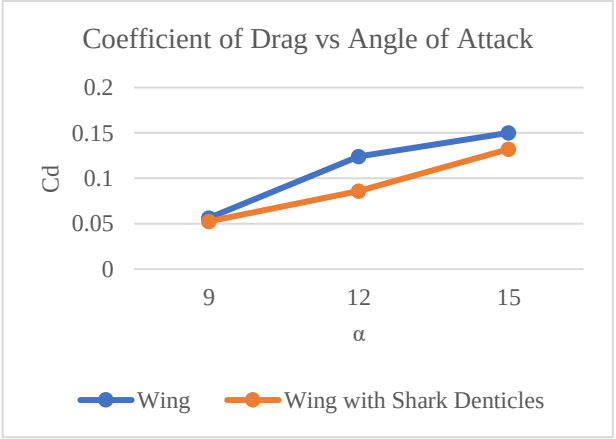

Graph 2. Cl vs α

6.4. Comparison-Table

6.4.1. Coefficient of Lift (C_L)

Table 4. Value of Cl

Angle of Attack	Wing	Wing with Shark Denticles
9°	0.39995214	0.4469837
12°	0.53073261	0.57194625
15°	0.44839777	0.55037211

6.4.2. Coefficient of Drag (C_D)

Table 5. Value of Cd

Angle of Attack	Wing	Wing with Shark Denticles
9°	0.05634903	0.052542038
12°	0.12400343	0.086071289
15°	0.15008865	0.13210165

7. Conclusion

After analyzing the wing at various angles of attack, it was discovered that when shark denticles are incorporated into the wing, the coefficient of lift increases dramatically, and the coefficient of drag decreases under subsonic conditions. Shark denticles have the potential to generate vortices and shift the flow from laminar to turbulent. However, experimental research may be required. Finally, more optimal combinations can be explored in future designs by changing the shark denticle dimensions, shark denticle position, and airfoil type.

References

[1] August G. Domel et al., "Shark Skin-Inspired Designs that Improve Aerodynamic Performance," *Journal of the Royal Society Interface*, vol. 15, no. 139, pp. 1-9, 2018. [CrossRef] [Google Scholar] [Publisher Link]

[2] S. Rajarajan et al., "Computational Flow Analysis overan Aircraft Wing by Incorporating Turbulent Flow Generators," *International Research Journal of Engineering and Technology (IRJET)*, vol. 7, no. 10, pp. 480-489, 2020. [Google Scholar] [Publisher Link]

[3] Prithvi Raj Arora et al., "Drag Reduction in Aircraft Model Using Elliptical Winglet," *The Journal of the Institution of Engineers, Malaysia*, vol. 66, no. 4, pp. 1-8, 2005. [Google Scholar] [Publisher Link]

[4] Sonia Chalia, and Manish Kumar Bharti, "Design and Analysis of Vortex Generator and Dimple over an Airfoil Surface to Improve Aircraft Performance," *International Journal of Advanced Engineering Research and Applications*, vol. 3, no. 4, pp. 173-181, 2017. [Google Scholar] [Publisher Link]

[5] Kousik Kumaar, and R. Maniiarasan, "Reduction of Skin Friction Drag in Wings by Employing Riblets," *International Journal of Engineering Research & Technology*, vol. 4, no. 7, pp. 1-6, 2015. [Google Scholar] [Publisher Link]

[6] Md. Fazle Rabbi, Rajesh Nandi, and Mohammad Mashud, "Induce Drag Reduction of an Airplane Wing," *American Journal of Engineering Research (AJER)*, vol. 4, no. 6, pp. 219-223, 2015. [Google Scholar] [Publisher Link]

[7] Rohith Indulekha Janardhanan et al., "A Research on Wind Tunnel on Drag Reduction in Aircraft Wing by Inducing Surface Roughness," *International Journal of Recent Technology and Engineering (IJRTE)*, vol. 8, no. 2S3, pp. 25-28, 2019. [CrossRef] [Publisher Link]

[8] Abubker Fadl et al., "A Numerical Investigation of the Performance of Wind Turbine Airfoils with Gurney Flaps and Airfoil Shape Alteration," *Journal of Engineering Science and Technology*, pp. 1-16, 2018. [Google Scholar] [Publisher Link]

[9] Frank M. White, *Viscous Fluid Flow*, McGraw-Hill Higher Education, pp. 1-614, 1991. [Google Scholar] [Publisher Link]

[10] John D. Anderson, *Computational Fluid Dynamics*, McGraw-Hill Education, 1995. [Google Scholar] [Publisher Link]

[11] Gurney Flap, 2022. [Online]. Available: https://en.wikipedia.org/wiki/Gurney_flap

[12] Wingtip Device, 2022. [Online]. Available: https://en.wikipedia.org/wiki/Wingtip_device

[13] Sanibel Sea School, 2022. [Online]. Available: https://www.sanibelseaschool.org/ blog/